Available online at www.sciencedirect.com
SCIENCE DIRECT®
Acta Materialia 53 (2005) 1041–1049
Acta MATERIALIA
www.actamat-journals.com

Quantitative determination of strain fields around Ni_4Ti_3 precipitates in NiTi

W. Tirry *, D. Schryvers

Electron Microscopy for Materials Science (EMAT) Physics Department, University of Antwerp (UA), Groenenborgerlaan 171, B-2020 Antwerp, Belgium

Received 9 July 2004; received in revised form 20 October 2004; accepted 31 October 2004
Available online 10 December 2004

Abstract

High-resolution transmission electron microscopy and image-processing techniques are used to measure the strain fields surrounding coherent Ni_4Ti_3 precipitates in an austenitic $Ni_{51}Ti_{49}$ matrix. Images are recorded in the $[1\ 1\ \bar{1}]_{B2}$ and the $[1\ 0\ \bar{1}]_{B2}$ zones, and the $\{1\ 1\ 0\}_{B2}$ interplanar spacings are used to determine the strain induced by both small (50 nm diameter) and large (300 nm diameter) precipitates. From these observations, the maximum strain in the surrounding matrix is mapped and identified as compressive or tensile. Interactions between strain fields of different precipitates are also investigated. A simple model for the observed strain is proposed and compared to the classical Eshelby solution for an ellipsoidal inclusion.

Keywords: Ni_4Ti_3 precipitation; NiTi; HREM; Strain field; Eshelby model

1. Introduction

NiTi alloys with near-equiatomic composition can exhibit shape memory and superelastic properties resulting from an austenite–martensite transformation under temperature change or applied stress. The properties of this transformation are strongly influenced by the presence of Ni_4Ti_3 precipitates in the B2 austenite matrix. The atomic structure and morphology of these precipitates have been investigated before [1–3] and it has been found that, due to the anisotropic change of the unit cell dimensions and lattice parameters, the precipitates form with a lens shape inside the cubic matrix. Their influence on the transformation temperatures and the occurrence of multiple step transformations were mainly investigated by differential scanning calorimetry (DSC) measurements and conventional transmission electron microscopy (TEM) [4–7]. When these precipitates are coherent or semi-coherent, which is the case for a diameter of the central disc up to 300 nm, they can act as nucleation centers for the formation of the R-phase [4,6]. This behavior is explained by the fact that the lattice mismatch between precipitate and matrix induces a stress field in the surrounding matrix. Also the change of Ni concentration in the matrix, due to the higher Ni content in the precipitates, can be expected to have an influence on the local transformation temperatures as is the case for concentration changes at the bulk level [4,8]. Larger precipitates lose their coherency with the matrix and the stress field is partially relaxed by the introduction of interface dislocations [9,10], though they can still act as nucleation centers for the R-phase [4]. In the coherent case, theoretical models are used to calculate which martensite variant is favored next to a particular precipitate, and to predict the morphology and growth of actual precipitate configurations consisting of several precipitates in close proximity and under the influence of an external applied stress [10–12].

* Corresponding author. Tel.: +32 3 265 32 63; fax: +32 3 218 02 57/265 32 57.
E-mail address: wim.tirry@ua.ac.be (W. Tirry).

1359-6454/$30.00
doi:10.1016/j.actamat.2004.10.049

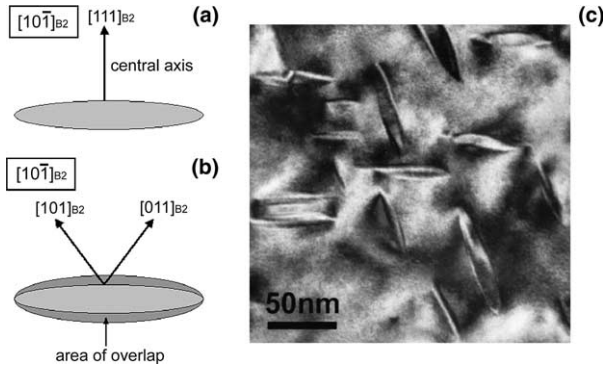

Fig. 1. Schematic drawing of the lens-shaped Ni_4Ti_3 in the two zones: (a) the $[1\,0\,\bar{1}]_{B2}$; (b) the $[1\,1\,\bar{1}]_{B2}$; (c) Typical BF image of Ni_4Ti_3 precipitates with surrounding strain contrast.

These calculations seem to confirm the experimental results, but they are typically based on a theoretical model for the stress field around the precipitate [10,13] as no localized experimental data on the nanoscale is available as yet. In the present work, high-resolution transmission electron microscopy (HRTEM) is used to measure the actual lattice deformations in the matrix around the Ni_4Ti_3 precipitates. To this end, the relative differences in interplanar spacings are determined by fast Fourier techniques applied to the HRTEM images obtained along two simple crystallographic zone directions of the matrix.

The cubic B2 structure of the matrix has a lattice parameter of $a = 0.30121$ nm [11], while for the precipitate the hexagonal description will be used with lattice parameters $a = b = 1.124$ nm and $c = 0.508$ nm [14]. As a result of the decrease in symmetry, eight precipitate variants are possible, the conventional orientation relationship being [1,14]:

$$(1\,1\,1)_{B2}//(0\,0\,1)_{H};\quad [3\,\bar{2}\,\bar{1}]_{B2}//[1\,0\,0]_{H}.$$

In this case the $[1\,1\,1]_{B2}$ direction corresponds to the normal to the central plane of the lens shaped precipitate. In this direction there is a 2.9% contraction in the precipitate relative to the matrix. TEM images indeed reveal this lens shape and conventional two-beam TEM contrast around them indicates the presence of a strain field, as already observed by Bataillard et al. [4]. Fig. 1(a) shows schematic top and side views of a precipitate while the two-beam bright field (BF) TEM image in Fig. 1(b) reveals the stress fields as strong contrast variation in the matrix surrounding the precipitates.

2. Experimental procedures

2.1. Sample preparation

Discs of thickness 300 μm are cut from a 3-mm diameter $Ni_{51}Ti_{49}$ rod and specifically heat treated to form coherent and semi-coherent Ni_4Ti_3 precipitates of different sizes. After homogenization treatment of 1 h at 950 °C in vacuum followed by water quenching, the samples are aged in vacuum for 4 h at 500 °C (sample A) or 450 °C (sample B) and again water quenched. Subsequently, the discs are mechanically ground, followed by double-jet electropolishing in a solution of 93% acetic acid and 7% perchloric acid at 6 °C. This solution yields well-polished samples without preferential etching between precipitates and matrix. The precipitates in samples A measure between 100 and 500 nm in diameter and are located mainly in the vicinity of grain boundaries and oxide or carbide particles. The precipitates in samples B are more finely distributed and their diameter is smaller than 100 nm.

2.2. Method for measuring interplanar spacings

High-resolution images are obtained with a top-entry JEOL 4000EX electron microscope equipped with a LaB_6 filament and operating at 400 kV. HRTEM micrographs are recorded on standard photographic plates in order to capture as much information as possible in a single image. Lattice deformations or strain are determined by measuring and comparing interplanar spacings at different positions in the HR image. The interplanar spacing of a crystallographic plane is measured by applying a fast Fourier transformation (FFT) to the digitized HR image. Then, the pixel distance is measured between the central spot (spatial frequency = 0) and that of the crystallographic plane under consideration.

As the expected deformations are relatively small, special care is required in order to obtain accurate and interpretable data. In practice, the micrographs are digitized with an appropriate scanner either directly from the negative or from an optical enlargement. The resulting image file is left uncompressed with original gray values. Possible artifacts introduced by the enlargement and/or scanner are compensated for by calibrating both procedures with images from undistorted matrices. In fact, distortions should only be measured at a perpendicular angle to the direction of motion of the scanner CCD array. Indeed, the discontinuous movement of the CCD array introduces false deformations in the direction of motion, which is why no two-dimensional displacement maps are made. Then, a window of (512, 512) pixels is moved over a constant distance (e.g. 128 pixels) as indicated in Fig. 2(a) and at each location the FFT is calculated. In order to avoid streaking in the FFT due to the sharp edges of the selection window, a mask filter is applied and the FFT is calculated as shown in Fig. 2(b). The matrix thus obtained is symbolized by FI.

To be able to accurately measure the distances between spots for each FFT window, their centers need